 doi:10.20944/preprints202007.0276.v1

Effects of four carboxyl-containing additives on imitation gold electroplating Cu-Zn-Sn alloys in an HEDP system

Lifeng Ding[=,1,3], Chongyan Chen[=,3], Qiang Li[2,*], Ruonan Wang[3], Qi Wang[1], Yanfeng Xue[1], Hongdao Li[1], Yulan Niu[1]

[1] Department of Chemistry and Chemical Engineering, Taiyuan Institute of Technology, Taiyuan 030008, PR China

[2] MicroNano System Research Center, College of Information and Computer & Key Laboratory of Advanced Transducers and Intelligent Control System of Ministry of Education and Shanxi Province, Taiyuan University of Technology, Taiyuan, 030024, PR China

[3] School of Chemical Engineering and Technology, North University of China, Taiyuan 030051, PR China

[=]These authors contributed equally to this work.

*Corresponding author: E-mail address: liqiang02@tyut.edu.cn.

Abstract: The requirements for using noncyanide imitation gold plating as decorative electroplating are increasing; thus, continuously improving the quality of the coating of the imitation gold plating and optimizing the coating process have become the current priority. In this work, hydroxyethylidene diphosphonic acid (HEDP) was used as the main complexing agent, $CuSO_4 \cdot 5H_2O$, $ZnSO_4 \cdot 7H_2O$ and $NaSnO_3 \cdot 3H_2O$ were the main salts, and NaOH and anhydrous sodium carbonate were used as the buffers to prepare the electroplating solution. Using sodium citrate (SC), sodium potassium tartrate (SS), sodium gluconate (SG), and glycerol (Gl) as four additives, the effects of the number of carboxyl groups on the properties of a Cu-Zn-Sn alloy coating were compared. The electrochemical analysis showed that Cu-Zn-Sn alloy codeposition occurred at -0.50 V vs. Hg|HgO. The scanning electron microscopy (SEM) results showed that the particle size of the coatings obtained with carboxyl-containing additives was more uniform than that obtained with the electroplating solution without additives. The X-ray fluorescence spectrometry (XRF) analysis revealed that the composition of the Cu-Zn-Sn alloy coating obtained by using SC as an additive in the electroplating solution was 89.75 wt% Cu, 9.61 wt% Zn, and 0.64 wt% Sn, and the color of the coating was golden yellow. The X-ray diffraction (XRD) pattern showed that the coating was a mixture of Cu, Cu_5Zn_8, CuSn, Cu_6Sn_5, and CuZn phases. The analysis of the electroplating solution by UV, IR and NMR spectroscopy methods indicates that the additives improve the coating by affecting the complexation reaction of metal ions. These results can provide technical and theoretical guidance for developing Cu-Zn-Sn ternary alloy

 doi:10.20944/preprints202007.0276.v1

electrodeposition technology with the new cyanide-free HEDP alkaline electroplating system.

Key Words: Imitation gold plating; Cu-Zn-Sn alloy; carboxyl-containing additives; HEDP system

1.Introduction：

Electroplating is one of the main methods used to coat industrially obtained metals on the surface of materials. In recent years, research on electroplated copper alloys has continued to develop [1-2]. Compared with the single metal coating, the ternary Cu-Zn-Sn alloy coating has a better flattening capability, brightness, luster, decorative effect and gliding property, leading to its widespread use [3]. In the earliest imitation gold plating techniques, cyanide was used as the main complexing agent, and the quality of the coating layer formed during the electroplating process was good. However, the cyanide-containing electroplating solution is toxic, and the waste liquid generated after electroplating is extremely harmful to the environment [4]. Thus, current research has been looking for a green and environmentally friendly cyanide-free electroplating solution.

Cyanide-free electroplating process systems are being developed. Among them, the pyrophosphate system [5], sorbitol system [6-8], EDTA system [9, 10], glycine system [11], mesylate system [12], gluconate system [13-14], HEDP system [15-16], triethanolamine system [17], citrate system [18-19], etc. have all achieved great results. HEDP is the main complexing agent in the electroplating solution of the HEDP system. HEDP can form stable water-soluble complexes with various metal ions, such as copper, zinc, and tin, and the resulting coating has fine and uniform crystals. In this system, the cost of the reaction material is low, the plating solution is simple and stable, and the corrosion extent of the plating production equipment is relatively small, which is more conducive to production. When HEDP is decomposed into various primary products by sunlight exposure, it can be considered a type of environmentally friendly complexing agent [20].

The traditional electroplating process uses additives to improve the quality of the coating. For example, L. Bonou [21] studied the effects of polyethylene glycol (PEG) and chloride on copper electrodeposition. When the additive PEG is used alone in the solution, the deposition efficiency decreases. The use of the additive Cl^- alone can promote copper deposition. When two additives are used at the same time, a copper reduction blocking reaction occurs. P.F.J.D. Leon [22] and others established an atomic model of Cu electrodeposition under nonequilibrium conditions. The

Preprints (www.preprints.org) | NOT PEER-REVIEWED | Posted: 13 July 2020 doi:10.20944/preprints202007.0276.v1

model pointed out that when an organic additive was present, the additive competed with Cu^{2+} in the solution, so the concentration at the electrode reaction interface was relatively stable. A. Dianat [23] studied the molecular dynamics of the additives PEG, bis(3-sulfopropyl)-disulfide (SPS) and chloride in copper metal deposition reactions by density functional theory and found that PEG inhibited the reaction function, while SPS and chloride played a promoting role. F. Lallemand [24] studied whether organic additives affect the deposition of metals through the current density and concluded that additives do not affect the mechanism of metal deposition but do affect the metal deposition rate. F.L.G. Silva [25] showed that using benzotriazole and cystine as additives can change the composition of the copper-zinc alloy and improve the corrosion resistance of the coating in the citrate electroplating Cu-Zn alloy system. L.F. Ding [26] studied the effects of four nitrogen-containing additives on the HEDP electroplating system and finally found that using ammonium fluoride as an additive can make the particles of the coating more uniform and produce coatings with better brightness and gloss.

So far, although many different types of electroplating systems and additives have been reported, they have only been described in terms of their effects, and their mechanisms have not been explained, which has restricted the development of using additives in imitation gold plating. In this work, the HEDP system was used. Four carboxyl-containing additives were added to the system and include sodium citrate ($Na_3C_6H_5O_7$, SC), sodium potassium tartrate ($C_4H_4KNaO_6$, SS), sodium gluconate ($C_6H_{11}NaO_7$, SG), and glycerol ($C_3H_8O_3$,Gl), where the number of carboxylic acid groups contained in these four molecules is 3, 2, 1, and 0, respectively.

The purpose of this work is to study the effects of four additives on the coating and the reaction mechanism. Therefore, the system uses the process parameters of L.F. Ding[26] in the previous study, such as current density, plating time, pH and so on. Scanning electron microscopy (SEM), X-ray fluorescence spectrometer (XRF) and X-ray diffraction (XRD) and other methods were used to characterize the morphology, composition and crystal morphology of the alloy coatings. The mechanism of complexation in the imitation gold of the electroplating solution was explored by UV, IR and NMR, which laid a certain theoretical foundation for future research on imitation gold plating mechanisms.

2. Experimental

2.1 Electroplating solution

Preprints (www.preprints.org) | NOT PEER-REVIEWED | Posted: 13 July 2020 doi:10.20944/preprints202007.0276.v1

The sequence in which the electroplating solution is prepared is crucial. First, the main complexing agent HEDP (60%, Shandong Youso Chemical Technology Co.) was measured. Then, $CuSO_4·5H_2O$ (≥ 99.0%, Tianjin Zhiyuan Chemical Reagent Co.), $ZnSO_4·7H_2O$ (≥ 99.5%, Tianjin Beichenfangzheng Reagent Factory), $Na_2SnO_3·3H_2O$ (≥ 98%, Tianjin Fuchen Chemical Reagent Factory) and Na_2CO_3 (≥ 99.8%, Tianjin Guangfu Technology Development Co.) were dissolved separately with a small amount of water, and the resulting solutions were then added to HEDP. To dissolve sodium stannate, which is insoluble in water and soluble in an alkaline solution, an appropriate amount of NaOH (≥96.0%, Tianjin Beichen Founder Reagent Factory) should be added. When adding a sodium carbonate solution, many bubbles will be generated, so the sodium carbonate solution needs to be slowly added with a plastic dropper. The electroplating solution without additives was used as the blank reference solution (BR). The main components in the BR electroplating solution are 0.18 mol/L $CuSO_4$, 0.06 mol/L $ZnSO_4$, 0.05 mol/L $Na_2SnO_3·3H_2O$, 100.0 mL/L HEDP, 25.0 g/L Na_2CO_3, and an appropriate amount of an NaOH solution to achieve a pH of 13.0-13.5. Finally, the different additives were added according to the solution requirements. Four carboxyl-containing additives, namely, SC (≥ 99.0%, Tianjin Beichenfangzheng Reagent Factory), SS (≥ 99.0%, Tianjin Beichenfangzheng Reagent Factory), SG (≥ 99.0%, Tianjin Beichenfangzheng Reagent Factory) and GL (≥ 99.0%, Tianjin Beichenfangzheng Reagent Factory) were selected for study. Water was purified using a water purification system (PALL Cascada II I 30, USA). All the reagents were of analytical grade.

2.2 Electroplating experiment

The electrolysis system used intelligent constant-current power (WJY- 30V/10A) as the power source. The electrocoating device consisted of an electroplating solution, a cathode plate, and an anode plate. The electroplating solution effective volume was 100 mL. The cathode was a 304 30 mm×70 mm×1.0 mm stainless steel plate, whose single-side effective area was 12.0 cm^2. The anode was made of $Cu_{0.7}Zn_{0.3}$ with 30 mm×70 mm×1.0 mm dimensions and had a single-side effective area of 15.0 cm^2. During the electrodeposition process, the temperature was maintained at 298 K, and the current density and electrolysis time were 3.5 $A·dm^{-2}$ and 60 s, respectively.

2.3 Characterization of the coating properties

The macroscopic morphology of the coatings was recorded by an optical camera (Canon A590 IS). The surface morphology of the coating was characterized by A-HITACHI-SU8010 scanning

Preprints (www.preprints.org) | NOT PEER-REVIEWED | Posted: 13 July 2020 doi:10.20944/preprints202007.0276.v1

electron microscope (SEM).The content of the alloying elements in the coatings was analyzed using an HMST-II-MZ X-ray fluorescence spectrometer (XRF). The images and spectra were collected with a 20 kV accelerating voltage. The phase analysis of the coatings was carried out by Bruker D_2 Phaser X-ray diffractioninstrument (XRD) (National Taiwan University of Science and Technology, China).

2.4 Characterization of the complexation reaction mechanisms

The electrochemical tests were conducted by a PARSTAT PMC1000 electrochemical workstation. A three-electrode system was used comprising, namely, the reference electrode (RE), which is a Hg|HgO electrode, the working electrode (WE) (Φ=10 mm, area=78.5 mm^2), which is made of 304 stainless steel, and the counter electrode (CE) (Φ=10 mm, area=78.5 mm^2), which is made of a $Cn_{0.7}Zn_{0.3}$ alloy. The materials of the WE and CE are commonly used in the electrocoating experiment. All the electrodes were finely polished and washed. To prevent the electrode area from fluctuating during testing, except for the effective area of the electrode, the remaining area was sealed by an insulating polymer. The scanning speed of the cyclic voltammetry test was 20 mV/s. Ultraviolet visible (UV–vis) spectroscopy was performed with a TU-1901 UV–vis spectrophotometer (Beijing Persee, China). Fourier transform infrared spectroscopy (FTIR) was performed by a Magna 550II FTIR spectrometer (Nicolet, USA). Nuclear magnetic resonance (NMR) was performed by an Avance ш 400M instrument (Bruker, Germany).

3.Results and discussion

3.1Effect of additives on the morphology of the coating

An optical camera was used to record the appearance of the plating tablet after electroplating. As shown in Fig.1, when there is no additive (BR) in the electroplating solution, the color of the plating tablet is uneven and is dark yellow and partially red. When the concentration of the additive SC was increased from 10 to 15 g/L, the color of the coating changed from dark yellow to golden yellow. When the SC concentration was 22 g/L, the color of the coating was uniform and golden yellow at this time. When the SC concentration is greater than 30 g/L, the coating is golden yellow, and part of it becomes increasingly black. When the concentration of the solution exceeds 40 g/L, a white precipitate will form after the solution is left for 24 hours, and the stability of the solution will deteriorate.

 doi:10.20944/preprints202007.0276.v1

When the amount of SS is 5 ~ 15 g/L, the color of the coating is uneven and light yellow. When the concentration is 20 g/L, the color of the coating is uniform and light yellow, and the stability of the solution is better at this time. When the amount of SS is 30, 35, or 40 g/L, the color of the coating is light yellow and partially blackened. When the SS concentration in the solution reaches 40 g/L and above, a white precipitate will appear after the solution is left for 24 hours, and the stability of the plating solution is poor.

When the amount of SG is 17.5~45 g/L, the color of the coating is uneven and is light yellow and partially red. When the amount of SG is less than 20 g/L, the stability of the plating solution is poor, white precipitates will form, and a wall hanging phenomenon will occur after long-term storage. When the amount of SG exceeds 40 g/L, a red precipitate will form in the solution. Therefore, the content of SG has a greater impact on the stability of the solution.

When the amount of Gl increased from 5 to 13 mL/L, the color of the coating gradually changed from dark yellow to yellow, and the gloss of the coating was relatively poor. When the amount of Gl is 15~20 mL/L, the color of the coating is even bronze. When the amount of Gl is more than 25 mL/L, the color of the coating is obviously black. When the amount of Gl was 30 mL/L, a yellow precipitate appeared after 24 hours of standing.

3.2 Effect of the additives on the surface micromorphology of the coating

It can be seen from Fig 2 that the BR coating surface is composed of spherical particles of varying sizes of 0.3-0.8 μm (Fig 2a). After adding 22 g/L SC to the BR, the coating obtained contains approximately 0.1-0.5 μm spherical particles (Fig 2b), and the particle size is relatively uniform. After adding 20 g/L SS to the BR, the particle size is approximately 0.1-0.5 μm, the particles are uniform, there are more fine particles (Fig 2c). When 30 g/L SG is added, the particle sizes on the surface of the coating are approximately 0.1-0.3 μm, but there are obvious cracks in the coating. (Fig 2d). When 20 mL/L Gl was added to the BR, the size of the spherical particles on the surface of the coating was approximately 0.2-0.5 μm, but local cracks appeared obviously (Fig 2e). Compared with that of the BR, the size of the crystal particles in the coating is reduced after adding the four additives, so additives with different numbers of carboxyl groups all have the effect of grain refinement.

3.3 Effect of the additives on the copper, zinc, and tin content in the coating

XRF was used to analyze the composition of the coating obtained in the presence of the four

 doi:10.20944/preprints202007.0276.v1

additives (Table 1). The coating alloy contained mainly copper, the zinc content was less than the copper content, and the tin content was trace. In the BR solution, the content of the copper, zinc, and tin components in the coating was 90.12 wt%, 9.46 wt%, and 0.42 wt%, respectively. At this time, the copper content in the coating is relatively high, which can explain why the abovementioned color is dark yellow but locally reddish. With the addition of the additives, the copper content in the coating alloys has been reduced. When the content ratio of copper, zinc and tin in the coating alloy changes, the color of the obtained coating is different. The comparison shows that when 22 g /L SC is added to the BR, the Cu content is reduced to 89.75 wt%, the Zn content is 9.61 wt%, and the Sn content is 0.64 wt%. At this time, this copper, zinc and tin ratio is the best ratio. The plating tablet appears to be uniform golden yellow. When 20 g/L SS was added to the BR, the copper, zinc and tin contents were adjusted slightly, but the plating tablet was a uniform light yellow color.

3.4 Effects of the additives on the phase composition of the coating

Fig 3 shows the X-ray diffraction pattern obtained by detecting the coating in the presence of the different additives in the plating solution. The results were compared to the expected patterns provided by the Committee on Powder Diffraction Standards (JCPDS). Cu (JCPDS 04-0836), Cu_5Zn_8 (JCPDS 71-0397), CuSn (JCPDS 44-1477), Cu_6Sn_5 (JCPDS 45-1488), CuZn (JCPDS 08-0349) and other crystals were observed [27-31]. For the phase containing Cu in the coating, the crystal diffraction peaks were mainly located at 2θ = 42.124°, 50.888°, 64.456°, and 90.888°. The 2θ positions of the diffraction peaks corresponding to the Cu_5Zn_8 phase are 42.124°, 44.504°, 75.172°, 82.348°, and 90.988°. The 2θ positions of the diffraction peaks corresponding to CuSn are 42.124°, 44.504°, 50.888° and 75.172°. The 2θ positions of the diffraction peaks correspond to Cu_6Sn_5 are 42.124°, 43.608°, 75.172° and 90.988°. The 2θ positions of the diffraction peaks corresponding to CuZn are 42.124°, 75.172°, and 82.348°.

Compare the four diffraction peaks with additives to the diffraction peaks of the BR, the 2θ position of the diffraction peak observed when 22 g/L SC was added was almost unchanged, but the height of the diffraction peak slightly changed. This shows that using SC as an additive does not affect the material composition of the coating alloy. When 20 g/L SS was added to the BR solution, the 2θ position of the diffraction peak did not change. When the additive is SG, the height of the diffraction peak at the 2θ position at 42.124° is significantly increased, and those

Preprints (www.preprints.org) | NOT PEER-REVIEWED | Posted: 13 July 2020 doi:10.20944/preprints202007.0276.v1

diffraction peaks are corresponding to CuSn, Cu_6Sn_5, CuZn, Cu_5Zn_8, and Cu. The diffraction peak at the 2θ position of 50.888° decreases, and this peak represents CuSn and Cu. The analysis shows that the Zn content in the coating alloy is relatively high at this time, which is consistent with the previous XRF test results. When 20 mL/L Gl was added, CuO (JCPDS 44-0706) diffraction peaks appeared at 41.492°, 93.576°, and 95.028°. This shows that the additives will affect the composition content of the coating, and using Gl as an additive will also affect the phase composition of the coating alloy.

Since XRF cannot directly test the oxygen content, the oxygen content in the coating is not discussed in Table 1. Therefore, use Energy Dispersive Spectrometer (EDS) to analyze the oxygen content in different coatings. The analysis showed that no oxygen could be detected in the coatings obtained from BR and additives containing SC, SS and SG. However, 0.57% oxygen was detected in the coating containing Gl additives. This is consistent with XRD analysis results.

3.5 Effect of the additives on the electrochemical reaction of the electrode

Electrochemical tests were performed on the electroplating solutions with different compositions. The results are shown in Fig 4. From the CV curve shown in 4a, it can be seen that the BR plating solution corresponds to the different cathode deposition peaks A, B, and C, which are located at -1.25 V, -1.10 V and -0.50 V vs. Hg|HgO, respectively. According to the literature, the deposition peak A at approximately -1.25 V vs. Hg|HgO represents the co-deposition peak of Cu and Sn, and the deposition peak B at -1.10 V vs. Hg|HgO mainly represents the Cu or Cu-containing compounds at the cathode. The cathode deposition peak C at -0.50 V vs. Hg|HgO represents the co-deposition precipitation peak of Cu-Zn-Sn. The potential D at -0.05 V vs. Hg|HgO is mainly the dissolution peak of the Cu anode. There is also an anode dissolution peak E at 1.0 V vs. Hg|HgO, which is the oxidation peak of water [32-37].

Fig 4a shows the CV curve obtained when different contents of SC were added to the solution. With the increase in the SC content, the intensities of the deposition peaks A, B, and C all increased gradually, indicating that increasing the amount of this additive is beneficial to metal deposition. The intensity of peak D increases, and peak E disappears gradually. This shows that the increase in the SC concentration in the plating solution is favorable to the dissolution of the anode, showing that the increase in the SC content is favorable to the plating experiments.

Fig 4b shows the CV curve obtained when SS was added to the solution. As the SS content

 doi:10.20944/preprints202007.0276.v1

increased, the cathode deposition peak A gradually disappeared, the intensity of peak B increased first and then decreased, and the intensity of peak C gradually increased. This shows that a certain amount of SS is favorable to metal deposition. With the increase in the SS content, the potential at the anode dissolution peak D is basically unchanged, the peak value gradually increases, and peak E gradually disappears, indicating that the increase in the content of the additives is favorable to anode dissolution. A comprehensive analysis of the deposition peaks A, B, and C theoretically found that when the SS content pf 20 g/L was most favorable for metal deposition.

Fig 4c shows the CV curve obtained when different contents of SG were added to the solution. When the SG content was increased from 17.5 g/L to 30 g/L, the deposition peaks A and B disappeared, and the intensity of peak C gradually increased. This shows that theoretically, compared with that in the BR, the Cu and Sn content in the coating is less and the Zn content, which is higher. This is consistent with the conclusions of XRF and XRD. The intensity and potential of dissolution peak D do not change, peak E disappears, and a new dissolution peak F appears at 0.45 V vs. Hg|HgO. This shows that the additive SG will also affect the dissolution of the anode. When the SG content continued to increase, the co-deposition peak of Cu-Zn-Sn shifted to the position of peak G of -0.02 V vs. Hg|HgO, indicating that the electrode reaction changed at this time. However, the potential of the dissolved peak D shifted to -0.25 V vs. Hg|HgO, the peak was almost unchanged, and peak E gradually disappeared.

Fig 4d shows the CV curve obtained when different contents of G1 was added to the solution. As the content of Gl increased, the intensity of peak A gradually decreased until peak A disappeared, peak B disappeared, and the intensity of peak C gradually increased. When the concentration of Gl is 20 mL/L, the height of cathode peak A is lower than the height of the corresponding cathode peak of the BR, peak B disappears, and the intensity of peak C is substantially unchanged. This theoretically shows that the Cu content in the coating is less than that in the BR at this time, which is consistent with the abovementioned conclusions of XRF and XRD. In addition, a hybrid peak H appears at a potential of -0.8 V vs. Hg|HgO, and the intensity of the peak gradually increases with an increase in the Gl content and reaches a maximum when the Gl content is 30 mL/L. Combined with the electroplating experiments, it was found that the increase in the Gl content will cause the surface of the coating to become black, so peak H may be a black oxide formed by deposition, which is not favorable to the co-deposition of the Cu-Zn-Sn

 doi:10.20944/preprints202007.0276.v1

ternary alloy. This is consistent with the abovementioned XRD analysis results. In the process of increasing the content of Gl, the intensity of peak D is basically unchanged, and peak E gradually disappears, indicating that Gl does not affect the dissolution of the anode.

In summary, the additives with more carboxyl groups will have a more significant positive effect on the electrodeposition of Cu-Zn-Sn alloys, and the content of each additive will also affect electrodeposition. Gl does not contain carboxyl groups. Increasing the content of Gl is not favorable to the co-deposition of the Cu-Zn-Sn alloy. When the content of SG is more than 30 g/L, the deposition potential of the cathode shifts, indicating that the electrode reaction changes. When the content of SS is more than 20 g/L, the intensity of the cathode deposition peak will decrease slightly. The SC additives contain the most carboxyl groups, which has the most favorable effect on the electrodeposition of Cu-Zn-Sn alloys. Combined with previous research, it was found that the content of additives not only affects deposition but also affects the stability of the plating solution. It can be concluded that the optimal contents of the four additives SC, SS, SG, Gl are 22 g/L, 20 g/L, 30 g/L, and 20 mL/L, respectively.

3.6 Effect of the additives on the UV-Vis spectrum

Fig 5a is the UV-Vis spectra of the plating solution containing different additives, and Fig 5b shows the maximum absorption wavelength of the five plating solutions. The maximum absorption peak of the BR was at 221 nm. After adding SC, SS, SG, and Gl to the electroplating solution, maximum absorption peaks were observed at 223 nm, 224 nm, 231 nm, and 226 nm, and it can be seen that the maximum absorption peaks have redshifted to different extents.

The reason for the redshift is not only the difference in the number of carboxyl groups in the four additives but also the number of hydroxyl groups in the four additives. Both carboxyl and hydroxyl groups are auxochromes, causing the wavelength of the maximum absorption peak to move in the direction of the long wave, causing a redshift. Among the additives, the total number of the two groups is the largest in the SG molecule, so the redshift is most obvious. However, comparing the UV spectra of the four additives, the position of the maximum absorption peak changes, and it is concluded that the UV absorption peak is mainly affected by the different additives. It is concluded that the maximum absorption peaks will be redshifted when additives are added to the plating solution. A proper redshift is beneficial to the formation of metal complex ions and the deposition of Cu-Zn-Sn ternary alloys.

 doi:10.20944/preprints202007.0276.v1

3.7 Effect of the additives on the FTIR spectrum

The analysis in Fig 5 shows that there is an absorption peak at 3370 cm^{-1} in the spectrum, and it is inferred that this peaks is a stretching vibration absorption peak attributed to the free and associated hydroxyl groups. The absorption peak at 3370 cm^{-1} appears because HEDP, NaOH, and the four additive molecules in the electroplating solution all contain hydroxyl groups. The absorption peak at 2450 cm^{-1} is the stretching vibration peak attributed to the C-H bond in the methyl ($-CH_3$) group in HEDP. When the additive is SG, the peak value of infrared absorption peak is the largest. When the additive is SS, the peak value are second. The absorption peaks at 1600 cm^{-1} and 1450 cm^{-1} are attributed to the asymmetric and symmetric stretching vibrations of the C=O bond in the carboxylate group in the solution. The absorption peak at 1100 cm^{-1} is attributed to the main complexing agent HEDP and the stretching vibration of the C-O bond in each additive molecule. When the additive is SS, the absorption peak value reaches the maximum at 1600 cm^{-1} and 1100 cm^{-1}. The weak peak at 980 cm^{-1} is attributed to the symmetric stretching vibration of the P-O bond in HEDP. Therefore, with the addition of carboxyl additives, the position of the infrared absorption peak of the plating solution is basically unchanged, but the height of the absorption peak changes. That is, a certain content of carboxyl additives does not have an effect on the infrared absorption peak of the electroplating solution but has an effect on the complexation of metal ions.

3.8 Effect of the additives on the NMR spectrum

To investigate the reaction mechanism of the additives used in this experiment, a deuterated reagent was used in place of deionized water to prepare the electroplating solution, and the ^1H nuclear magnetic resonance spectrum was obtained. See Fig 7. The chemical shifts of the test absorption peaks are summarized in Table 2. It can be seen from the data that the peak $1^{\#}$ with a chemical shift of 4.74 ppm is the absorption peak corresponding to H in the deuterated reagent [38]. HEDP has three kinds of H atoms with different chemical environments: H in HO-P-, H in the HO-C- group, and H in the $-CH_3$ group. The chemical shifts of 3.70 ppm and 3.68 ppm of peak $2^{\#}$ are formed by H in the HO-C- group. The absorption peak $4^{\#}$ at a chemical shift of 1.40 ppm was generated by H in HO-P-. The absorption peak $3^{\#}$ at chemical shifts of 1.28, 1.24, 1.20 ppm is a triplet formed by H in the $-CH_3$ group, and the splitting is caused by the two Ps on the same carbon. It can be known from Table 2 that when the additives of 22 g/L SC, 20 g/L SS, and 30 g/L

Preprints (www.preprints.org) | NOT PEER-REVIEWED | Posted: 13 July 2020 doi:10.20944/preprints202007.0276.v1

SG were added, the peak chemical shift and peak shape do not change, and only the peak height changes. This is because the additives will affect the complexation reaction of the metal ions, meaning that the peak-producing groups cannot rotate freely, and the height of the absorption peak changes. The peak height can reflect the reaction intensity of the metal ions and complexing agent to a certain extent. When the additive is 20 mL/L Gl, the chemical shift is 2.47 ppm, and peak $3^{\#}$ appears at 2.34 ppm. Peak $3^{\#}$ is a peak attributed to the two symmetric -CH_2- groups in the molecular structure. The analysis shows that the four additives with different numbers of carboxyl groups will all react with metal ions.

3.9 Reaction mechanism of electroplating

This work mainly studies the electroplating process of electroplating coating alloy in HEDP system. The main salts are $CuSO_4 \cdot 5H_2O$, $ZnSO_4 \cdot 7H_2O$ and $Na_2SnO_3 \cdot 3H_2O$, the complexing agent is HEDP, and the buffering agents are sodium hydroxide and anhydrous sodium carbonate. The molecular formula of the main complexing agent HEDP was $C(CH_3)(OH)(PO_3H_2)_2$. The molecular structure was characterized to contain two phosphonic acid groups and five hydroxyl groups, often expressed as H_4L, which can form a six-membered ring chelated with metal ions. At a pH of 13.0-13.5, HEDP mainly exists in the form of L^{4-}. When the pH is greater than 13.0, HEDP mainly exists in the form of L^{4-} [39-41].

According to the literature, when the pH is greater than 13, the main copper ion salt in the electroplating solution exists as a large amount of $Cu(OH)_4^{2-}$ and a small amount of CuL_2^{6-}. The electrodeposition reaction of $Cu(OH)_4^{2-}$ was as follows:

$$Cu(OH)_4^{2-} + 2e^- \rightarrow Cu + 4OH^- \quad (1)$$

The electrodeposition of CuL_2^{6-} is completed by a two-step discharge process:

$$CuL_2^{6-} \rightarrow CuL^{2-} + L^{4-} \quad (2)$$

and $$CuL^{2-} + 2e^- \rightarrow Cu + L^{4-} \quad (3)$$

Zinc ions exist in the electroplating solution as a large amount of $Zn(OH)_4^{2-}$ and a small amount of $(ZnLOH)^{3-}$ and $Zn(OH)_3^-$. The electrodeposition reaction of $Zn(OH)_4^{2-}$ was as follows:

$$Zn(OH)_4^{2-} + 2e^- \rightarrow Zn + 4OH^- \quad (4)$$

The tin ions in the electroplating solution exist as a large amount of $Sn(OH)_3^-$ and a small amount of $SnL(OH)_2^{4-}$. The electrodeposition reaction was as follows:

$$Sn(OH)_3^- + 2e^- \rightarrow Sn + 3OH^- \quad (5)$$

 doi:10.20944/preprints202007.0276.v1

The analysis of the electroplating solution by electrochemical, UV, IR, and NMR spectroscopy methods found that these four carboxyl-containing additives would result in electrolytic ionization and electroreduction in the solution and affect the microstructure of the coating. These additive can act as auxiliary complexing agents to react with metal ions in the plating solution, thereby improving the stability of the complex ions in the plating solution and promoting the progress of metal ions co-deposition. The higher the carboxyl group content, the more obvious its effect, specifically when the additive is SC, which is most conducive to the dissolution of the copper anode. These four additives do not change the electrochemical mechanism of the reaction. Each metal ion in the strong alkaline solution still exists in the form of $Cu(OH)_4^{2-}$, $Zn(OH)_4^{2-}$, and $Sn(OH)_3^-$, and electrodeposition reactions occur.

4. Conclusion

In this work, the effect of the number of carboxyl groups on the coatings co-deposited with different phases was investigated. It was concluded by an SEM analysis that with the addition of carboxyl-containing additives, the particle size of the alloy particles was reduced, and the more carboxyl-containing additives added, the better the effect. The XRF results show that when the electroplating solution contains the SC additive with the highest carboxyl number content, the obtained coating contains 89.75 wt% Cu, 9.61 wt% Zn, and 0.64 wt% Sn. At this time, the content ratio of Cu/Zn/Sn in the coating is optimized, and its appearance is golden yellow. The XRD analysis showed that the coating was a mixture of Cu, Cu_5Zn_8, CuSn, Cu_6Sn_5, and CuZn phases. The electrochemical analysis showed that metal co-deposition occurs at -0.50 V vs. Hg|HgO, and using a certain amount of carboxyl groups as additives can promote metal co-deposition. UV, IR and NMR spectroscopy methods were used to study the solution and showed that additives with different carboxyl numbers can improve the coating because the carboxyl groups affect the complexation of the metal ions in the solution.

Acknowledgements

This work was supported by the National Natural Science Foundation of China (NSFC51604180), Cultivate Scientific Research Excellence Programs of Higher Education Institutions in Shanxi (CSREP2019KJ038), General Project of Shanxi Province Key R & D Plan (Social Development Field, 201903D321068), the Applied Basic Research Programs of Science and Technology Department of Shanxi Province (201701D221036), Scientific and Technologial Innovation Programs of Higher Education Institutions in Shanxi (2019L0235).

 doi:10.20944/preprints202007.0276.v1

Reference

[1] Hyeon, G. M.; Dong, J. K.; Jun, H. P. Comparison of Tensile and Fatigue Properties of Copper Thin Film Depending on Process Method. Appl.Sci-basel.2020, 10, 2-11.

[2]Seo, H.; Park, H. S.; Kim, S. E.; Two-Step Plasma Treatment on Sputtered and Electroplated Cu Surfaces for Cu-To-Cu Bonding Application. Appl. Sci-basel. 2019, 9, 3535.

[3] Yang, S.C.; Ho, C.E.; Chang, C.W.; Kao, C.R. Strong Zn concentration effect on the soldering reactions between Sn-based solders and Cu. J. Mater. Res. 2006, 21, 2436-2439.

[4] Piccinini, N.; Ruggiero, G. N.; Baldi, G.; Robotto, A. Risk of hydrocyanic acid release in the electroplating industry. J. Hazard. Mater. 2000, 7, 395-407.

[5] Clauwaert, K.; Binnemans, K.; Matthijs, E.; Fransaer, J. Electrochemical studies of the electrodeposition of copper-zinc-tin alloys from pyrophosphate electrolytes followed by selenization for CZTSe photovoltaic cells. Electrochim. Acta. 2016, 188, 344-355.

[6] Almeida, M.R.H.D.; Barbano, E.P.; Carvalho, M.F.D.; Tulio, P.C.; Carlos, I.A. Copper-zinc electrodeposition in alkaline-sorbitol medium: Electrochemical studies and structural, morphological and chemical composition characterization. Appl. Surf. Sci. 2015, 333, 13-22.

[7] Rubin, W.; Oliveira, E.M.D.; Carlos I.A. Study of the influence of a boric–sorbitol complex on Zn-Mn electrodeposition and on the morphology, chemical composition, and structure of the deposits. J. Appl. Electrochem. 2012, 42, 11-20.

[8] Barbosa, L.L.; Finazzi, G.A.; Tulio, P.C.; Carlos, I.A. Electrodeposition of zinc–iron alloy from an alkaline bath in the presence of sorbitol. J. Appl. Electrochem. 2008, 38, 115-125.

[9] E.P. Barbano; Oliveira, G.M.D.; Carvalho, M.F.D.; Carlos, I.A. Copper-tin electrodeposition from an acid solution containing EDTA added. Surf. Coat. Tech. 2014, 240, 14-22.

[10] Almeida, M.R.H.D.; Barbano, E.P.; Zacarin, M.G.; Brito, M.M.D.; Tulio P.C.; Carlos I.A. Electrodeposition of CuZn films from free-of-cyanide alkaline baths containing EDTA as complexing agent. Surf. Coat. Tech. 2016, 287, 103-112.

[11] Ballesteros, J.C.; Chainet, E.; Ozil, P.; Trejo G.; Meas, Y. Initial stages of the electrocrystallization of copper from non-cyanide alkaline bath containing glycine. J. Electroanal. Chem. 2010, 645, 94-102.

[12] Pewnim, N.; Roy, S. Electrodeposition of tin-rich Cu–Sn alloys from a methanesulfonic acid electrolyte. Electrochim. Acta. 2013, 90, 498-506.

[13] Rudnik, E.; Wloch, G. Studies on the electrodeposition of tin from acidic chloride–gluconate solutions. Appl. Surf. Sci. 2013, 265, 839-849.

[14] Gougaud, C.; Rai, D.; Delbos, S.; Elisabeth, C.; Daniel, L. lectrochemical studies of one-step electrodeposition of Cu-Sn-Zn layers from aqueous electrolytes for photovoltaic applications. J. Electrochem. Soc. 2013, 160, 485-494.

[15] Zheng, J.W.; Chen, H.B.; Cai, W.; Qiao, L.; Ying, Y.; Li, W.C.; Yu, J.; Jiang, L.Q. Reaction mechanisms of copper electrodeposition from 1-hydroxyethylidene-1, 1-diphosphonic acid (HEDP) solution on glassy carbon. A study on electroplating of zinc nickel alloy with HEDP plating bath. Che. Mater. Sci. Eng. B. 2017, 224, 18-27.

[16] Wang, Z.L.; Yang, Y. X.; Zhang, J.B.; Zhu H.; Chen, Y. R. A study on electroplating of zinc nickel alloy with HEDP plating bath. Russ. J. Electrochem. 2006, 42, 22-26.

[17] Whang, T.J.; Hsieh, M.T.; Kao Y.C.; Lee S. J. A study of electrodeposition of CuInSe2 thin films with triethanolamine as the complexing agent. Appl. Surf. Sci. 2009, 225, 4600-4605.

[18] Slupska M.; Ozga, P. Electrodeposition of Sn-Zn-Cu alloys from citrate solutions.

Electrochim. Acta. 2014, 141, 149-160.

[19] Ashworth, M.A.; Wilcox, G. D.; Higginson, R.L. An investigation into zinc diffusion and tin whisker growth for electroplated tin deposits on brass. J. Electron. Mater. 2014, 43, 1005-1016.

[20] Boswell, H. D.; Marsh, J. M.; Olshavsky, M A.; Park, J. S. Compositions suitable for the treatment of hair comprising chelants and methods for reducing oxidative hair damage. 2003.

[21] Bonou, L.; Eyraud, M.; Denoyel, R.; Massiani Y. Influence of additives on Cu electrodeposition mechanisms in acid solution: direct current study supported by non-electrochemical measurements. Electrochim. Acta. 2003, 21, 4139-4148.

[22] Leon, P.F.J.D.; Albano,E.V.; Salvarezza, R.C. Interface dynamics for copper electrodeposition: the role of organic additives in the growth mode. Phys. Rev. E. 2002, 66, 042601.

[23] Dianat, A.; Yang, H.; Bobeth, M.; Cuniberti, G. DFT study of interaction of additives with Cu(111) surface relevant to Cu electrodeposition. J. Appl. Electrochem. 2018, 48, 211-219.

[24] Lallemand, F.; Ricq, L.; Wery, M.; Bercot, P.; Pagetti, J. The influence of organic additives on the electrodeposition of iron-group metals and binary alloy from sulfate electrolyte. Appl. Surf. Sci. 2004, 228, 326-333.

[25] Silva, F.L.G.; Lago, D.C.B.D.; Elia, E.D.; Senna L.F. Electrodeposition of Cu–Zn alloy coatings from citrate baths containing benzotriazole and cysteine as additives. J.Appl. Electrochem. 2010, 40, 2013-2022.

[26] Ding, L.F.; Liu, F.; Cheng, J.; Niu, Y.L. Effects of four N-based additives on imitation gold plating. J. Appl. Electrochem. 48 (2018) 175-185.

[27] Joint Committee on Powder Diffraction Standards; JCPDS (2000), Powder Diffraction File-PDF-2, Database Sets 1-49. ICDD, Pennsylvania, (CDROM).

[28] Xue, L.; Fu, Z.; Yu, Y.; Tao, H.; Yu, A. Three-dimensional porous Sn–Cu alloy anode for lithium-ion batteries. Electrochim. Acta. 2010, 55, 7310-7314.

[29] He, X.C.; Shen, H.L.; Wang, W.; Pi, J.H.; Hao, Y.; Shi, X.B. Synthesis of Cu2ZnSnS4 films from co-electrodeposited Cu-Zn-Sn precursors and their microstructural and optical properties. Appl. Surf. Sci. 2013, 282, 765–769.

[30] Hsieh, M.F.D.; Tsai, Y.T.; Su, R.W.; Sun, C.J. Electrodeposition of CuZn from chlorozincate ionic liquid: from hollow tubes to segmented nanowires. J. Phys. Chem. C. 2014, 118, 22347-22355.

[31] Carvalho, M.F.D.; Barbano, E.P.; Carlos, I.A. Electrodeposition of copper-tin-zinc ternary alloys from disodium ethylenediaminetetraacetate bath. Surf. Coat. Tech. 2015, 262, 111-122.

[32] Carvalho, M.F.D.; Barbano, E.P.; Carlos, I.A. Influence of disodium ethylene diaminetetraacetate on zinc electrodeposition process and on the morphology, chemical composition and structure of the electrodeposits. Electrochim. Acta. 2013, 109, 798-808.

[33] Shin, S.; Park, C.; Kim, C.; Kim, Y.; Park, S.; Lee, J H. Cyclic voltammetry studies of copper, tin and zinc electrodeposition in a citrate complex system for CZTS solar cell application. Curr. Appl. Phys. 2016, 16, 207-210.

[34] Zhao, X.; Zhang, J.J.; Qu, J.H. Photoelectrocatalytic oxidation of Cu-cyanides and Cu-EDTA at TiO2 nanotube electrode. Electrochim. Acta. 2015, 180, 129-137.

[35] Ballesteros, J.C.; Chaînet, E.; Ozil, P.; Trejo, G.; Meas, Y. Initial stages of the electrocrystallization of copper from non-cyanide alkaline bath containing glycine. J. Electroanal. Chem. 2010, 645, 94-102.

 doi:10.20944/preprints202007.0276.v1

[36] Kulyk, N.; Cherevko, S.; Chung, C.H. Copper electroless plating in weakly alkaline electrolytes using DMAB as a reducing agent for metallization on polymer films. Electrochim. Acta. 2012, 59, 179-185.

[37] Jung, M.; Lee, G.; Choi, J. Electrochemical plating of Cu-Sn alloy in non-cyanide solution to substitute for Ni undercoating layer. Electrochim. Acta. 2017, 241, 229-236.

[38] Schah-Mohammedi, P.; Shenderovich, I.G.; Detering, C.; Limbach, H.H.; Tolstoy, P.M.; Smirnov, S.N.; Golubev, N.S. Hydrogen/Deuterium-Isotope effects on NMR chemical shifts and symmetry of homoconjugated hydrogen-bonded ions in polar solution. J. Am. Chem. Soc. 2000, 122, 12878-12879.

[39] Sergienko, V. S. Specific structural features of 1-hydroxyethane-1,1-siphosphonic acid (HEDP) and its salts with organic and alkali-metal cations. Crystallogr. Rep. 2000, 45, 64-70.

[40] Pecequilo, V.; Cristiane. Study of copper electrodeposition mechanism from a strike alkaline bath prepared with 1-hydroxyethane-1,1-diphosphonic acid through cyclic voltammetry technique. Electrochim. Acta. 2010, 55, 3870-3875.

[41] Zheng, J.; Chen, H.; Cai, W.; Qiao, L. Reaction mechanisms of copper electrodeposition from 1-hydroxyethylidene-1,1-diphosphonic acid (HEDP) solution on glassy carbon. Che. Mater. Sci. Engin. B. 2017, 224, 18-27.

 doi:10.20944/preprints202007.0276.v1

Preprints (www.preprints.org) | NOT PEER-REVIEWED | Posted: 13 July 2020 doi:10.20944/preprints202007.0276.v1

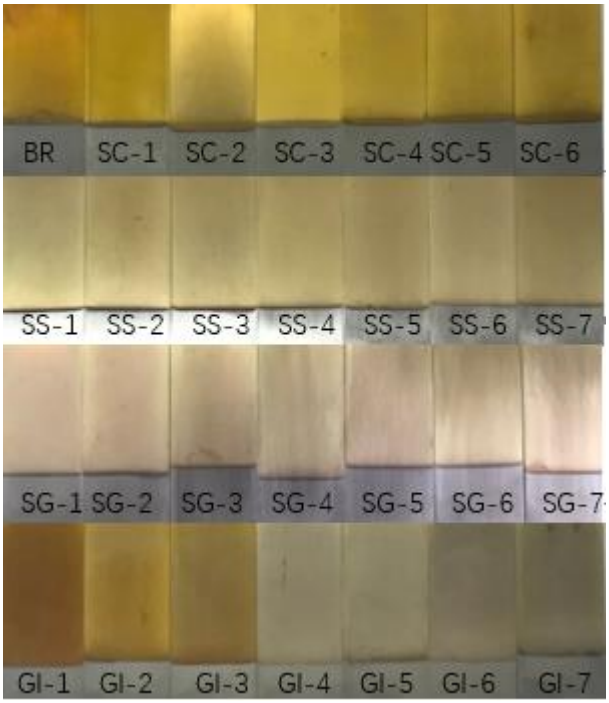

Fig 1. Effect of additives on the morphology of the coating

BR:0 SC:10、15、22、30、35、40g/L. SS:5、10、15、20、30、35、40 g/L.

SG:17.5、20、25、30、35、40、45 g/L. Gl:5、10、13、15、20、25、30ml/L.

Preprints (www.preprints.org) | NOT PEER-REVIEWED | Posted: 13 July 2020 doi:10.20944/preprints202007.0276.v1

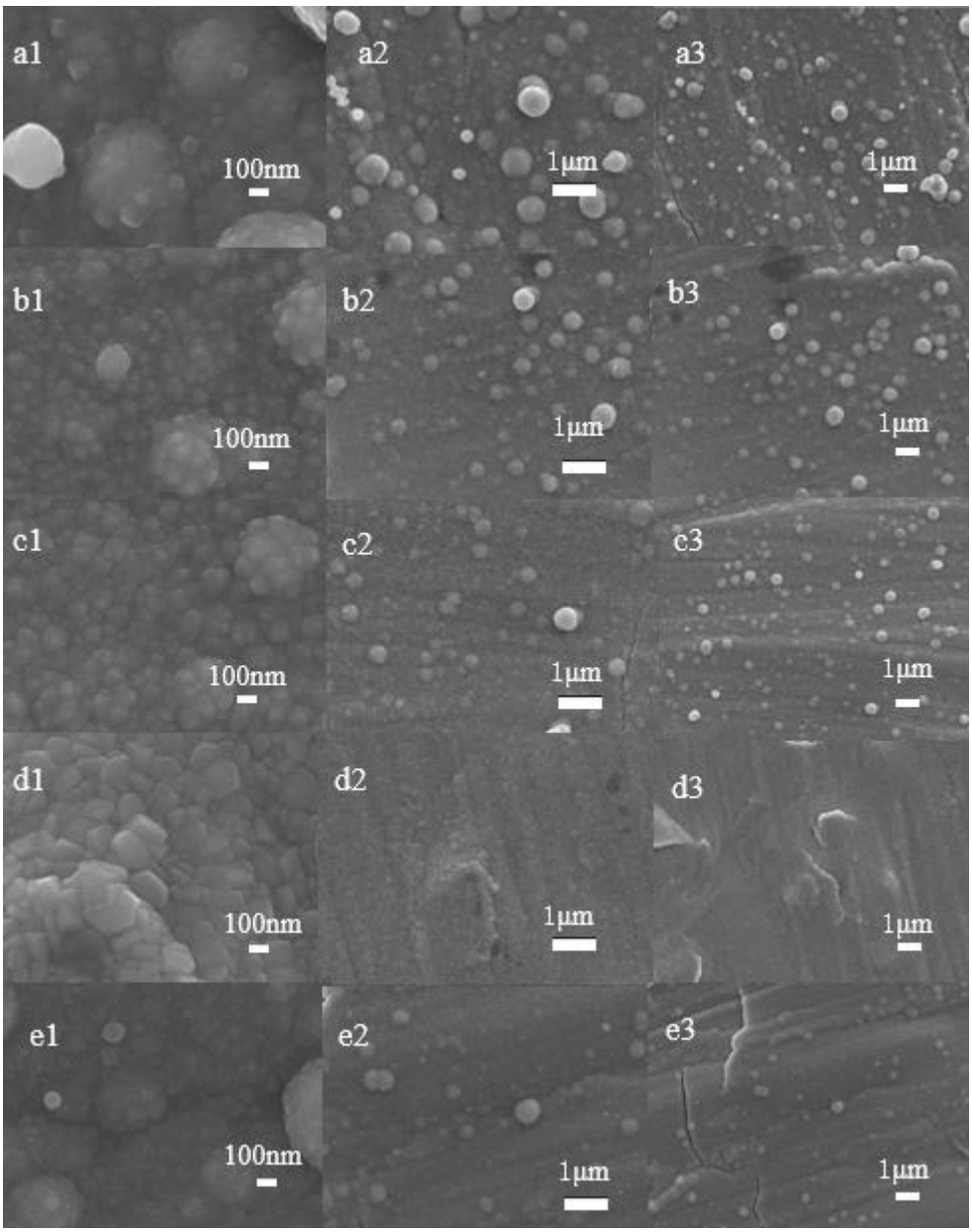

Fig 2. Effect of the additives on the surface micromorphology of the coating

(a_1), (a_2), (a_3): BR. (b_1), (b_2) and (b_3) :BR + 22g/L SC. (c_1), (c_2) and (c_3) :BR +20g/L SS. (d_1), (d_2) and (d_3) :BR + 30g/L SG. (e_1), (e_2) and (e_3) :BR + 20mL/L Gl.

Preprints (www.preprints.org) | NOT PEER-REVIEWED | Posted: 13 July 2020 doi:10.20944/preprints202007.0276.v1

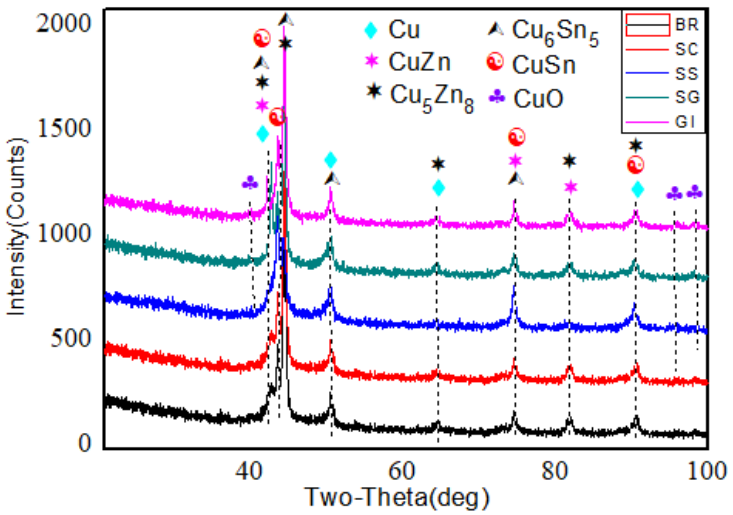

Fig 3. Effects of the additives on the phase composition of the coating

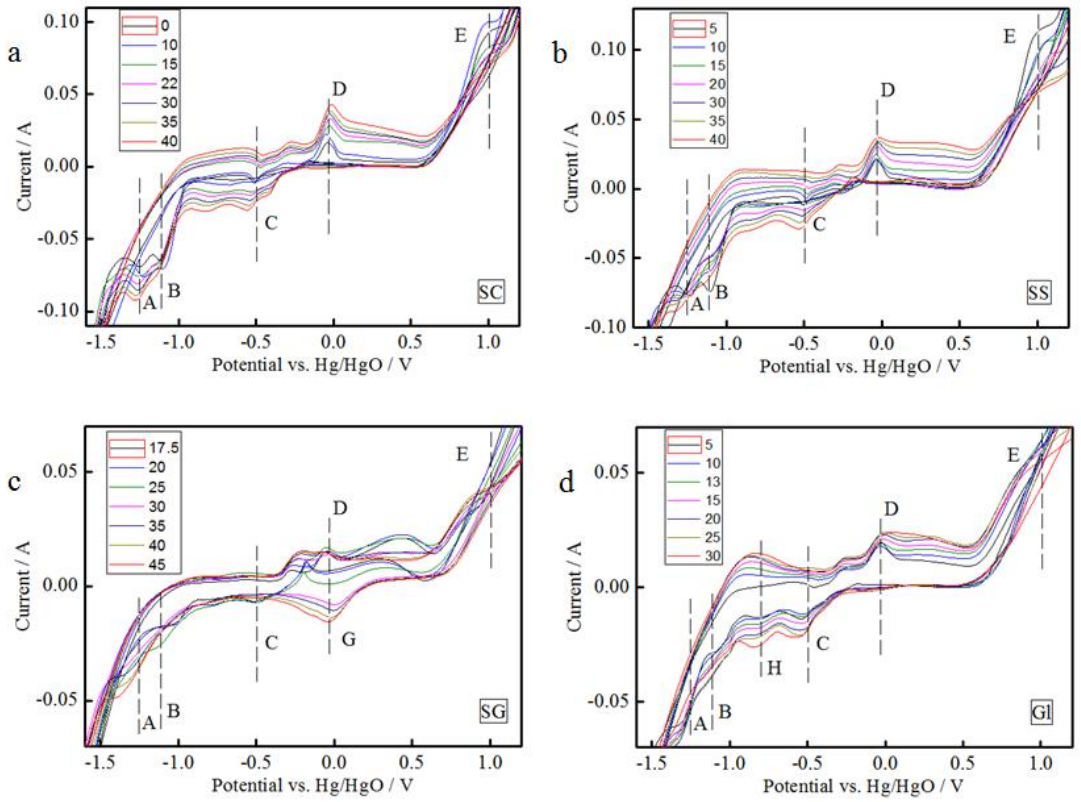

Fig 4. Effect of the additives on the electrochemical reaction of the electrode

Preprints (www.preprints.org) | NOT PEER-REVIEWED | Posted: 13 July 2020 doi:10.20944/preprints202007.0276.v1

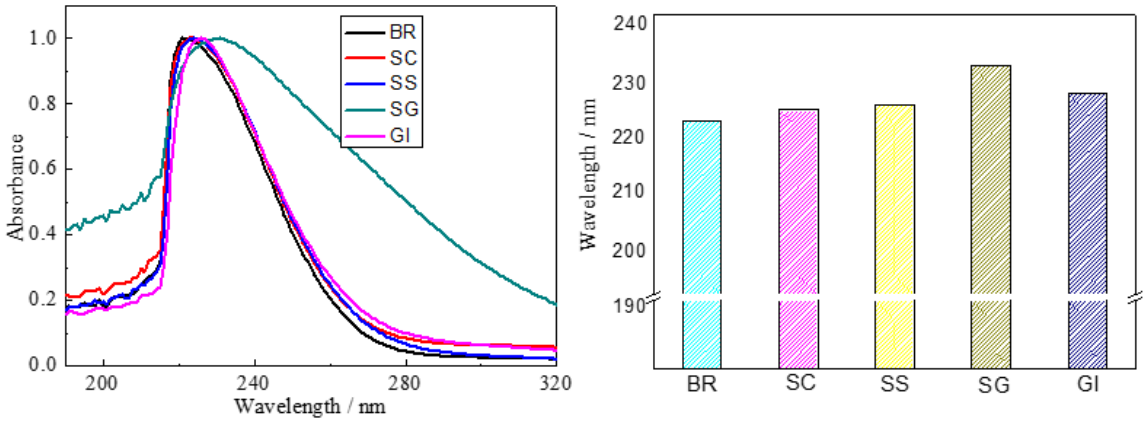

Fig 5. Effect of the additives on the UV-Vis spectrum

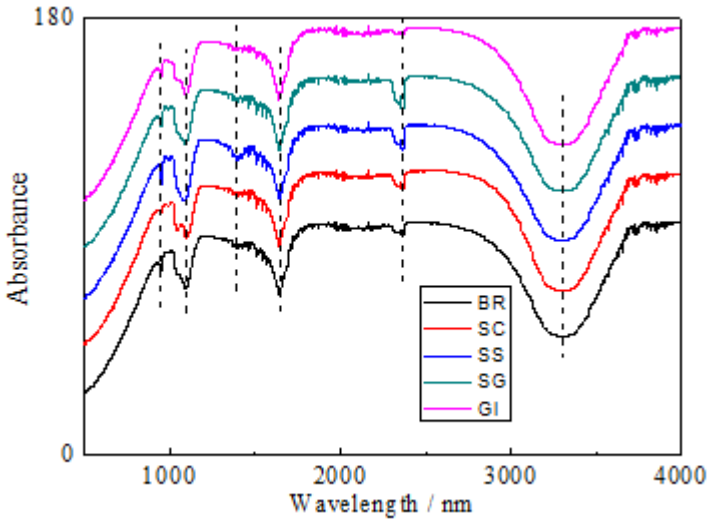

Fig 6. Effect of the additives on the FTIR spectrum

Preprints (www.preprints.org) | NOT PEER-REVIEWED | Posted: 13 July 2020 doi:10.20944/preprints202007.0276.v1

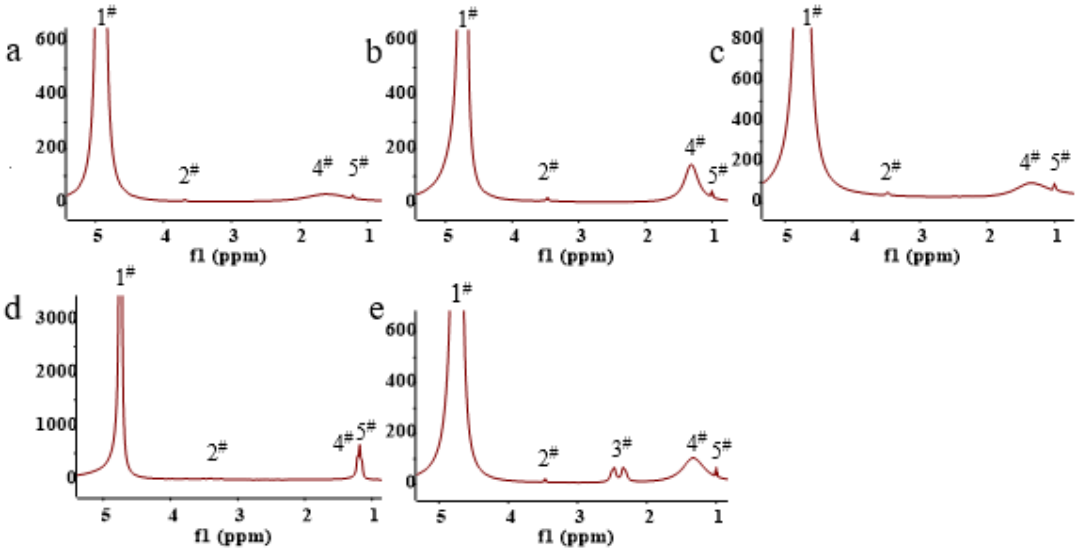

Fig 7. Effect of the additives on the NMR spectrum

Preprints (www.preprints.org) | NOT PEER-REVIEWED | Posted: 13 July 2020 doi:10.20944/preprints202007.0276.v1

Table 1. Content of each metal in the coating

sample composion	Cu (wt%)	Zn (wt%)	Sn (wt%)
BR	90.12	9.46	0.42
BR + 22g/L SC	89.75	9.61	0.64
BR + 20g/L SS	90.05	9.42	0.53
BR + 30g/L SG	84.56	15.07	0.37
BR + 20mL/L Gl	88.85	10.68	0.47

Table 2. NMR detection of the different additives in the electroplating solutions

Sample composition	chemical shift (ppm)				
	peak 1#	peak 2#	Peak 3#	peak 4#	peak 5#
BR	4.74	3.70,3.68		1.40	1.20,1.21,1.23
BR+ 22g/L SC	4.74	3.37,3.46		1.31	1.02,1.00,0.98
BR+ 20g/L SS	4.74	3.48		1.35	1.00
BR+ 30g/L SG	4.74	3.42,3.32		1.32	1.22,1.18,1.15
BR+ 20mL/L Gl	4.74	3.48,3.46	2.47，2.34	1.33	1.02,1.00,0.98

Preprints (www.preprints.org) | NOT PEER-REVIEWED | Posted: 13 July 2020 doi:10.20944/preprints202007.0276.v1

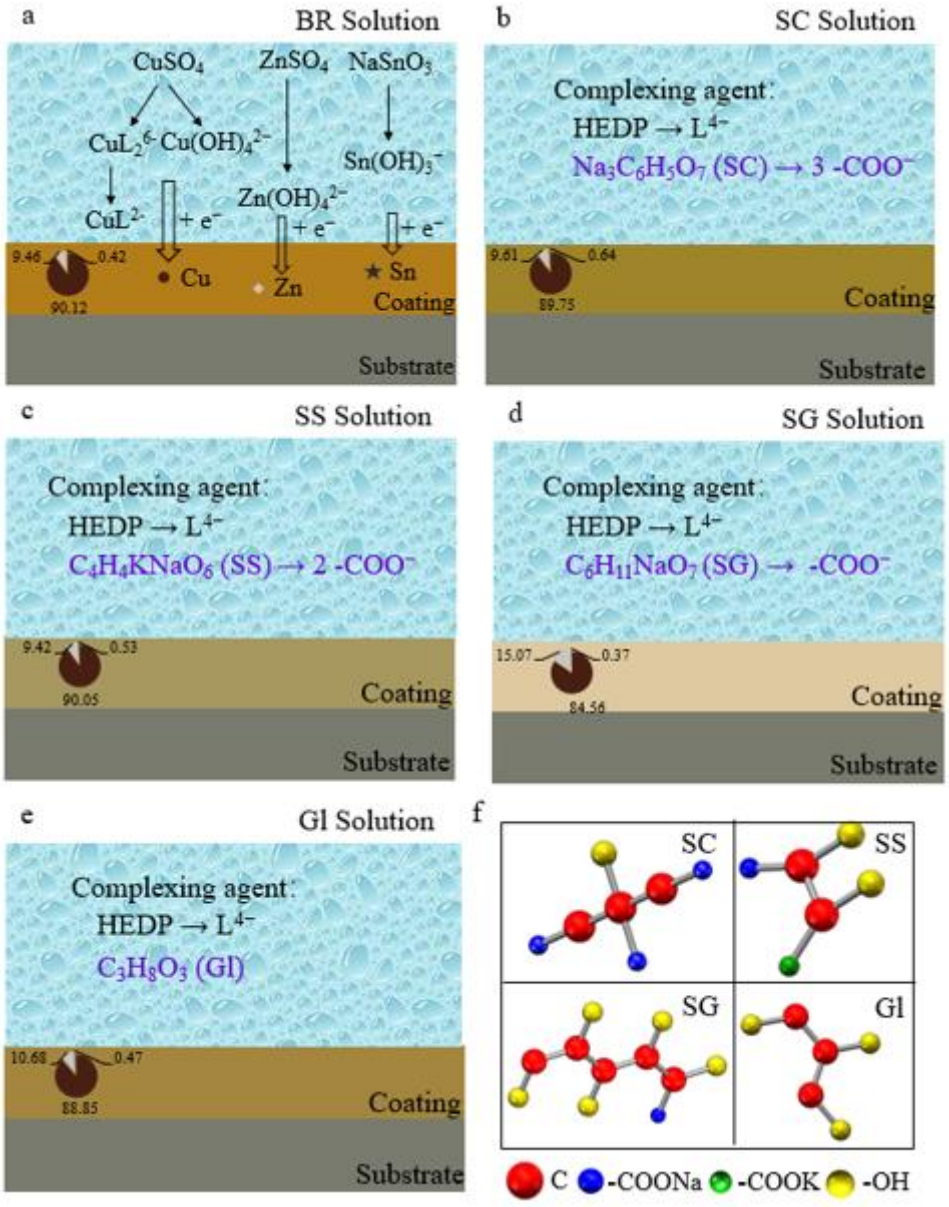

Graphic Abstract